Tight Bounds on the Effective Complex Permittivity of Isotropic Composites and Related Problems

Christian Kern,[1,*] Owen D. Miller,[2] and Graeme W. Milton[1]

[1] *Department of Mathematics, University of Utah, Salt Lake City, Utah 84112, USA*

[2] *Department of Applied Physics and Energy Sciences Institute, Yale University, New Haven, Connecticut 06511, USA*

(Received 4 June 2020; revised 22 August 2020; accepted 5 October 2020; published 30 November 2020)

Almost four decades ago, Bergman and Milton independently showed that the isotropic effective electric permittivity of a two-phase composite material with a given volume fraction is constrained to lie within lens-shaped regions in the complex plane that are bounded by two circular arcs. An implication of particular significance is a set of limits to the maximum and minimum absorption of an isotropic composite material at a given frequency. Here, after giving a short summary of the underlying theory, we show that the bound corresponding to one of the circular arcs is at least almost optimal by introducing a certain class of hierarchical laminates. In regard to the second arc, we show that a tighter bound can be derived using variational methods. This tighter bound is optimal as it corresponds to assemblages of doubly coated spheres, which can be easily approximated by more realistic microstructures. We briefly discuss the implications for related problems, including bounds on the complex polarizability.

DOI: 10.1103/PhysRevApplied.14.054068

I. INTRODUCTION

Composite materials can exhibit effective "metamaterial" properties that are quite different from those of their underlying constituents [1–3] but the range of such emergent properties is not limitless. The effective permittivity of a two-phase isotropic composite with fixed volume fraction is constrained by the "Bergman-Milton" (BM) bounds [4–8] to lie within two circular arcs in the complex plane, yet the feasibility of approaching the extreme permittivity values—or, conversely, finding tighter bounds—has remained largely an open question. In this paper, we resolve this question: we show that one of the arcs is nearly attainable via hierarchical laminates, we show that the other arc can be replaced by a tighter bound that can be derived by variational methods, and we identify assemblages of doubly coated spheres as structures that can achieve the extreme permittivity values at the new boundary. To design the hierarchical laminates that reach or approach the first arc, we start with five classes of microstructures that have previously been identified as optimal over narrow regions of BM bounds. Forming laminates from these microstructures leads to the identification of additional optimal microstructures and to broad coverage near the entirety of the first arc. To replace the second arc, we embed a rank-2 transformed permittivity tensor into a rank-4 effective tensor and use the "Cherkaev-Gibiansky transformation" [9] together with the "translation method" [10–14] to maximally constrain the tensor values, adapting techniques used for related questions on the effective complex bulk modulus [15]. These results provide a comprehensive understanding of possible effective metamaterial permittivities. For applications targeting extreme response, such as maximal absorption, these results refine the global bounds on what is possible and offer powerful microstructure design principles toward achieving them.

In the following, we study the effective-permittivity problem in the quasistatic regime for isotropic microstructures that are made from two isotropic materials (phases). We assume that the volume fractions f_1 and $f_2 = 1 - f_1$ of the two phases are given, which is typically the problem of interest in applications in which the weight, or cost, of one of the phases is an issue. However, our results are not limited to fixed volume fractions, as the corresponding results for arbitrary volume fractions follow as a simple corollary.

The quasistatic regime corresponds to the assumption that the structures are periodic and that the wavelength and attenuation lengths in the phases and the composite are much longer than the unit cell of periodicity. In this case, one can use the quasistatic equations (see Sec. 11.1 in Ref. [1])

$$\mathbf{d} = \varepsilon\mathbf{e}, \quad \nabla \times \mathbf{e} = 0, \quad \nabla \cdot \mathbf{d} = 0, \quad \varepsilon = \chi\varepsilon_1 + (1-\chi)\varepsilon_2, \tag{1}$$

*kern@math.utah.edu

where $\mathbf{d}(\mathbf{x})$ and $\mathbf{e}(\mathbf{x})$ are complex periodic vector fields, with the real parts of $\mathbf{d}(\mathbf{x})e^{-i\omega t}$ and $\mathbf{e}(\mathbf{x})e^{-i\omega t}$ representing the electric displacement field and the electric field, respectively, $\chi(\mathbf{x})$ is the periodic characteristic function, that takes the value 1 in phase 1 and 0 in phase 2, and ε_1 and ε_2 are the (frequency-dependent) complex electric permittivities of the two materials. Letting $\langle\cdot\rangle$ denote a volume average over the unit cell of periodicity, we may solve these equations for any value of $\langle\mathbf{e}\rangle$ (provided that $\varepsilon_1/\varepsilon_2$ is finite, nonzero, and non-negative). Then, since $\langle\mathbf{d}\rangle$ depends linearly on $\langle\mathbf{e}\rangle$, we may write

$$\langle\mathbf{d}\rangle = \varepsilon_*\langle\mathbf{e}\rangle, \tag{2}$$

which defines the effective complex electric permittivity, ε_*.

The goal is then to find the range that ε_* takes as the geometry, i.e., $\chi(\mathbf{x})$, varies over all periodic configurations with an isotropic effective permittivity that have the prescribed volume fraction f_1 of phase 1. The geometries that realize (or almost realize) the maximum and minimum values of the imaginary part of ε_* are those that show (close to) the maximum and minimum amount of absorption of an incoming plane wave or a constant static applied field. It is not only the imaginary part of ε_* that is of interest, as both the real and imaginary parts are of importance in determining the effective refractive index and the transmission and reflection at an interface. If there is a slow variation (relative to the local periodicity) in the microstructure, the resulting variations in $\varepsilon_*(\mathbf{x})$ can be used to guide waves.

Substantial progress on this problem was made about four decades ago when bounds on the effective complex electric permittivity were derived [4–8] (see also Chaps. 18, 27, and 28 in Ref. [1]), which have become known as the "Bergman-Milton" (BM) bounds. The BM bounds comprise bounds for several different restrictions on the geometry of the structure, including the problem that we are studying here, i.e., bounds for structures with isotropic effective permittivity (which includes, for example, all geometries with cubic symmetry) and fixed volume fractions.

Originally, the BM bounds were derived on the basis of the analytic properties of ε_* as a function of ε_1 and ε_2. Bergman, in his pioneering work [16], had recognized the analytic properties but erroneously assumed that the function would be rational for any periodic geometry (a checkerboard is a counterexample [17,18]; see also Chap. 3 in Ref. [1]) and that if the equations did not have a solution for a prescribed average electric field, then they would have a solution for a prescribed average displacement field (a square array of circular disks having $\varepsilon_1 = -1$ inside the disks and $\varepsilon_2 = 1$ outside the disks is a counterexample in which neither has a solution) [18]. An argument that avoided these difficulties by approximating the composite by a discrete network of two electric impedances has been put forward [6] and, later, the analytic properties have been rigorously established by Golden and Papanicolaou [19].

The BM bounds can also be used in an inverse fashion, i.e., to obtain information about the composition of a material from a measurement of its effective properties. If we know that a composite material is made from two phases with known permittivities, we can use the BM bounds to obtain bounds on the volume fraction from a measurement of its effective permittivity [20,21]. In essence, one has to find the range of values of the volume fraction for which the measured value of the effective permittivity lies in the lens-shaped region.

We remark, in passing, that the analytic method is also useful for bounding the response in the time domain for a given time-dependent applied field (that is not at constant frequency) [22]. This approach is more useful for the equivalent antiplane elasticity problem, since the typical relaxation times are much longer.

Furthermore, the analytic properties extend to the Dirichlet-to-Neumann map governing the response of bodies containing two or more phases, not just in quasistatics but also for wave equations (at constant frequency) (see Chaps. 3 and 4 in Ref. [23]).

Before discussing the BM bounds in more detail, we briefly consider the analytic properties of the electric permittivity as a function of frequency [24,25], which are a result of the fundamental restrictions imposed by causality and passivity. Causality, i.e., the fact that the electric displacement field at a certain point in time depends on the electric field at prior times only, implies that the frequency-dependent permittivity, $\varepsilon(\omega)$, is an analytic function in the upper halfplane. If, additionally, the material is passive, i.e., if it does not produce energy, the imaginary part of the permittivity is non-negative for positive real frequencies. These properties, which in mathematical terms mean that the permittivity can be expressed via a Stieltjes or a Nevanlinna-Herglotz function [26–29], have far-reaching and not immediately intuitive consequences. The Kramers-Kronig relations, which express the real (dispersive) part of the permittivity in terms of its imaginary (absorptive) part and vice versa, constitute a well-known example. Moreover, the analytic properties lead to sum rules, i.e., relations connecting integral quantities involving the permittivity with its static and high-frequency behavior, which prove useful in a variety of applications. For example, sum rules have been used to derive bounds on broadband cloaking in the quasistatic regime [29] and on dispersion in metamaterials [30]. As one may expect, such considerations are not limited to electromagnetics but apply to transfer functions of passive linear time-invariant (LTI) systems in general [28].

In order to derive the BM bounds, one uses the fact that the analytic properties extend to the permittivity as a function of the constituent phases [19]. More precisely,

one uses the fact that $\varepsilon_*(\varepsilon_1,\varepsilon_2)$ is a homogeneous function of ε_1 and ε_2 (so it suffices to consider the function with $\varepsilon_2 = 1$) and $f(z) = \varepsilon_*(1/z, 1)$ is a Stieltjes function of z, thus having the integral representation

$$f(z) = \alpha + \frac{\beta}{z} + \int_0^\infty \frac{d\mu(t)}{t+z}, \tag{3}$$

for all z not on the negative real axis of the complex plane, where α and β are non-negative real constants and $d\mu$ is a non-negative measure on $(0,\infty)$. Depending on the assumptions about the geometry of the composite, the Stieltjes function satisfies different constraints [16,19]: First, for an arbitrary, potentially anisotropic composite material, the Stieltjes function satisfies

$$f(1) = 1. \tag{4}$$

Second, if the volume fraction of phase 1 in the composite, f_1, is prescribed, the Stieltjes function additionally satisfies

$$\left.\frac{df(z)}{dz}\right|_{z=1} = -f_1. \tag{5}$$

Third, if the composite is assumed to be isotropic, the Stieltjes function additionally satisfies

$$\left.\frac{d^2 f(z)}{dz^2}\right|_{z=1} = 2f_1 - \frac{2f_1 f_2}{3}. \tag{6}$$

The goal is then to determine the sets of values that the function $f(z)$ and, hence, the effective permittivity (or any diagonal element of the effective permittivity tensor) attains as the geometry, i.e., the measure $d\mu$, is varied while being subject to the first constraint (anisotropic composites), the first and the second constraint (anisotropic composites with fixed volume fraction), and all of the constraints (isotropic composites with fixed volume fraction).

It can be shown that mappings between these sets are realized by linear fractional transformations [19,31] (see also Chap. 28 in Ref. [1]). As these transformations map generalized circles (circles or straight lines) onto generalized circles, one obtains a set of nested bounds, the BM bounds, that confine the effective permittivity to lens-shaped regions bounded by circular arcs. It should be pointed out that in the larger arena of Stieltjes functions, lens-shaped bounds corresponding to the BM bounds and their generalizations have a long history (see, e.g., Refs. [32–35]).

The BM bounds for an isotropic composite material with fixed volume fraction confine ε_* to lie within the following lens-shaped region in the complex plane. One side is the circular arc traced by

$$\varepsilon_*^+(u_1) = f_1\varepsilon_1 + f_2\varepsilon_2 - \frac{f_1 f_2(\varepsilon_1-\varepsilon_2)^2}{3(u_1\varepsilon_1 + u_2\varepsilon_2)}, \tag{7}$$

as u_1 is varied so that $u_1 \geq f_2/3$ and $u_2 \geq f_1/3$ while keeping $u_1 + u_2 = 1$ [6]. The essential feature of this formula is that it has only one pole (resonance) at finite negative values of the ratio $\varepsilon_1/\varepsilon_2$. On the other side is the circular arc traced by

$$\varepsilon_*^-(u_1) = \left(\frac{f_1}{\varepsilon_1} + \frac{f_2}{\varepsilon_2} - \frac{2f_1 f_2(1/\varepsilon_1 - 1/\varepsilon_2)^2}{3(u_1/\varepsilon_1 + u_2/\varepsilon_2)}\right)^{-1}, \tag{8}$$

as u_1 is varied so that $u_1 \geq 2f_2/3$ and $u_2 \geq 2f_1/3$ while keeping $u_1 + u_2 = 1$ [6]. The two circular arcs meet at the points

$$\begin{aligned}\varepsilon_*^+(f_2/3) = \varepsilon_*^-(2f_2/3) &= \varepsilon_2 + \frac{3f_1\varepsilon_2(\varepsilon_1-\varepsilon_2)}{3\varepsilon_2 + f_2(\varepsilon_1-\varepsilon_2)},\\ \varepsilon_*^+(1-f_1/3) = \varepsilon_*^-(1-2f_1/3) &= \varepsilon_1 + \frac{3f_2\varepsilon_1(\varepsilon_2-\varepsilon_1)}{3\varepsilon_1 + f_1(\varepsilon_2-\varepsilon_1)}.\end{aligned} \tag{9}$$

When ε_1 and ε_2 are real, the lens-shaped region collapses to an interval between these two points, thus giving the well-known Hashin-Shtrikman bounds [36]. For this reason, the BM bounds have sometimes been called the complex Hashin-Shtrikman bounds, which might be considered an occurrence of Stigler's law [37], as Hashin and Shtrikman had nothing to do with their derivation. The two points given in Eq. (9) correspond to the Hashin-Shtrikman assemblages of coated spheres that fill all space, each being identical to one another, apart from a scale factor [36]. Illustrations of such a coated-sphere assemblage and its columnar counterpart, the coated-cylinder assemblage, are shown in Fig. 1.

In Ref. [6], Milton identified microstructures that attain three additional points on the arc $\varepsilon_*^+(u_1)$. His key idea was to look for microstructures that have only one pole, as this is the characteristic feature of the bound (7). If one finds such a microstructure with a diagonal anisotropic effective tensor $\boldsymbol{\varepsilon}_*$, then, by forming a so-called Schulgasser laminate [38], one can obtain a composite with isotropic effective permittivity $\mathrm{Tr}(\boldsymbol{\varepsilon}_*)/3$. As described in detail in Sec. 22.2 of Ref. [1], the corresponding lamination scheme is based on the following observation. Consider two materials with diagonal permittivity tensors and the same principal permittivity in one direction, such as when one is a 90° rotation of the other about this direction. If these two materials are laminated along this direction, then the effective permittivity tensor of the laminate is just an arithmetic mean of the permittivity tensors of the two materials. By successively applying this idea on widely separated length

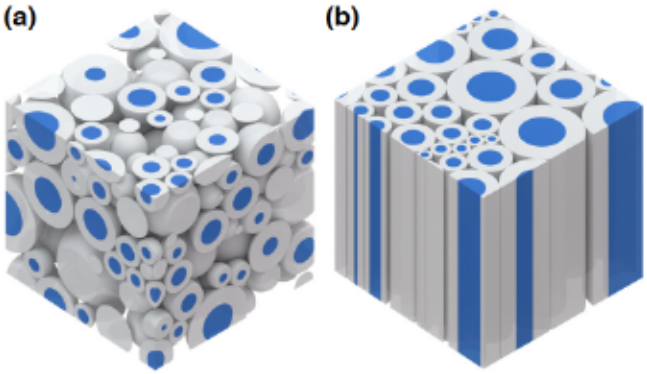

FIG. 1. Schematic illustrations of the Hashin-Shtrikman assemblages of coated spheres (a) and coated cylinders (b). The spheres (cylinders) are identical except for a scaling factor and fill all space.

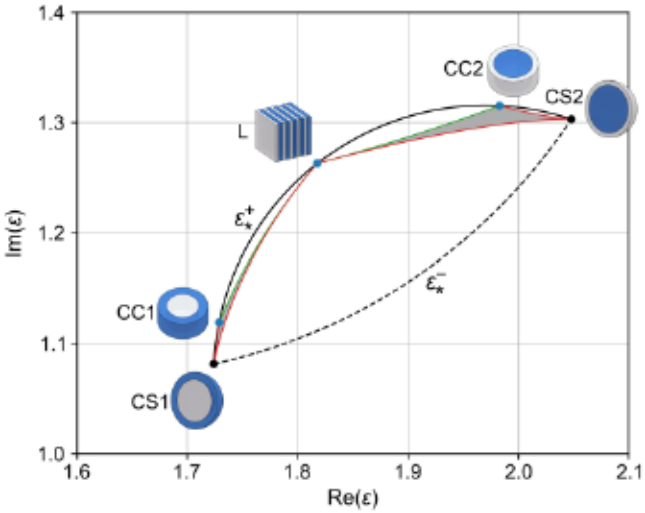

FIG. 2. An illustration of the Bergman-Milton bounds for an isotropic composite material with fixed volume fraction. The effective complex permittivity is constrained to a lens-shaped region bounded by the two circular arcs $\varepsilon_*^+(u_1)$ and $\varepsilon_*^-(u_1)$. The five points on the arc $\varepsilon_*^+(u_1)$ correspond to the two Hashin-Shtrikman assemblages of coated spheres with phase 1 and phase 2 as the core material, CS1 and CS2, respectively, Schulgasser laminates of the two Hashin-Shtrikman assemblages of coated cylinders, CC1 and CC2, and a Schulgasser laminate formed from a simple rank-1 laminate, L. The gray-shaded region corresponds to Schulgasser laminates formed from assemblages of coated ellipsoids. It is bounded by Schulgasser laminates of coated elliptical cylinders and coated spheroids, corresponding to the green and red curves, respectively. The parameters are $\varepsilon_1 = 0.2 + 1.5i$, $\varepsilon_2 = 3 + 0.4i$, and $f_1 = 0.4$.

scales, starting from the anisotropic material with diagonal effective tensor $\boldsymbol{\varepsilon}_*$, one obtains a hierarchical laminate with isotropic effective permittivity $\mathrm{Tr}(\boldsymbol{\varepsilon}_*)/3$. If one takes $\boldsymbol{\varepsilon}_*$ to be the effective permittivity of a simple laminate, an assemblage of coated cylinders with a core of phase 1 and a coating of phase 2, and an assemblage of coated cylinders with a core of phase 2 and a coating of phase 1, this results in the effective permittivities $\varepsilon_*^+(f_2)$, $\varepsilon_*^+(f_2/2)$, and $\varepsilon_*^+(1-f_1/2)$, respectively, which, as illustrated in Fig. 2, all lie on the arc $\varepsilon_*^+(u_1)$.

These three microstructures, as well as the Hashin-Shtrikman coated-sphere assemblage, can be seen as special cases of Schulgasser laminates formed from assemblages of coated ellipsoids (those having only one pole). The effective permittivity tensor, $\boldsymbol{\varepsilon}_*$, of such assemblages can be obtained from the following formula [1]:

$$f_1\varepsilon_1(\boldsymbol{\varepsilon}_* - \varepsilon_2\mathbf{I})^{-1} = \varepsilon_2(\varepsilon_1 - \varepsilon_2)^{-1}\mathbf{I} + f_2\mathbf{M}, \qquad (10)$$

where $\mathbf{I}$ is the identity matrix and $\mathbf{M}$ is a matrix that depends on the depolarization tensors of the ellipsoids. As the shape and orientation of the ellipsoids is varied, $\mathbf{M}$ ranges over all positive-semidefinite symmetric matrices with $\mathrm{Tr}(\mathbf{M}) = 1$ (see Sec. 7.8 in Ref. [1]). If one chooses the coordinate system such that its axes coincide with the principal axes of the ellipsoids, $\mathbf{M}$ is a diagonal matrix. The range of effective permittivities of Schulgasser laminates formed from such assemblages is illustrated in Fig. 2. It is bounded by Schulgasser laminates formed from assemblages of coated elliptical cylinders, $\mathbf{M} = (\alpha, 1-\alpha, 0)$ with $\alpha \in [1/2, 1]$, and coated spheroids, $\mathbf{M} = (\alpha, \alpha, 1-2\alpha)$ with $\alpha = [0, 1/2]$.

The first main thrust of this paper is to show that there are hierarchical laminate geometries that attain, depending on the volume fraction, two or three more points on the arc $\varepsilon_*^+(u_1)$ and other hierarchical laminates, which typically come extremely close to attaining the entire arc. This result shows that any improved bound, if it exists, typically can only be marginally better than Eq. (7). Note that while we are focussing on bounds on the complex permittivity, similar conclusions almost certainly apply to the attainability of four related bounds: those coupling the two effective permittivities $\varepsilon_* = \varepsilon_*(\varepsilon_1, \varepsilon_2)$ and $\widetilde{\varepsilon}_* = \varepsilon_*(\widetilde{\varepsilon}_1, \widetilde{\varepsilon}_2)$ for given real positive values of ε_1, ε_2, $\widetilde{\varepsilon}_1$, and $\widetilde{\varepsilon}_2$ [16]; those associated bounds of Beran [39] in the form simplified by Milton [40] and Torquato and Stell [41,42] (that can be obtained by taking the limit as $\widetilde{\varepsilon}_1 \to \widetilde{\varepsilon}_2 \to 1$; see Ref. [43]) that correlate, at fixed volume fraction, $\boldsymbol{\varepsilon}_*$ with a geometric parameter ζ_1, or $\zeta_2 = 1 - \zeta_1$, that can be calculated from the three-point correlation function giving the probability that a triangle positioned and oriented randomly in the composite has all three vertices in phase 1 or, respectively, phase 2; those bounds on the complex effective bulk modulus [15] of an isotropic composite of two isotropic elastic phases; and those bounds that couple the effective conductivity with the effective bulk modulus [44] when the conductivities and elastic moduli of the phases are real. For all of these problems, the same five microstructures attaining the points $\varepsilon_*^+(f_2/3)$, $\varepsilon_*^+(f_2)$, $\varepsilon_*^+(f_2/2)$, $\varepsilon_*^+(1-f_1/2)$ and

$\varepsilon_*^+(1-f_1/3)$ have also been shown to attain the relevant bounds [7,15,43,44].

It was noted in Ref. [6] that the formula given in Eq. (8) does not satisfy the phase interchange inequality

$$\varepsilon_*(\varepsilon_1,\varepsilon_2)\varepsilon_*(\varepsilon_2,\varepsilon_1) \geq \varepsilon_1\varepsilon_2 \tag{11}$$

of Schulgasser [45], which holds when ε_1 and ε_2 are real and non-negative. Consequently, it has been suggested that the bound (8) is nonoptimal [6]. In fact, using this inequality, an improved bound has been obtained by Bergman [8]. However, the inequality is itself nonoptimal and a tighter inequality,

$$\frac{\varepsilon_*(\varepsilon_1,\varepsilon_2)\varepsilon_*(\varepsilon_2,\varepsilon_1)}{\varepsilon_1\varepsilon_2} + \frac{\varepsilon_*(\varepsilon_1,\varepsilon_2)+\varepsilon_*(\varepsilon_2,\varepsilon_1)}{\varepsilon_1+\varepsilon_2} \geq 2, \tag{12}$$

has been proposed [6] and partially proved [43], with an error in the proof corrected in Refs. [46,47]. As remarked in Ref. [6], this inequality holds as an equality for any assemblage of multicoated spheres where all multicoated spheres in the assemblage are identical apart from a scale factor. In two dimensions, the Schulgasser inequality, Eq. (11), holds as an equality not just for coated-disk assemblages but for any geometry in which the (two-dimensional) effective permittivity is isotropic [48]. The identity can be used to improve the bounds on the complex permittivity for isotropic two-dimensional composites of two isotropic phases or, equivalently, the transverse conductivity of a three-dimensional geometry where the conductivity does not vary in the axial direction and the resulting bounds [5,6] are attained by assemblages of doubly coated disks. (The claim in Ref. [4] that these bounds are wrong was unfounded.) This suggests that the doubly-coated-sphere assemblage (with the appropriate phase at the central core) may in fact correspond to an optimal bound on the effective complex permittivity, replacing the bound (8). Additional evidence is that for the four related bounding problems mentioned above, the doubly-coated-sphere assemblages make their appearance in attaining a bounding curve.

The second main thrust of this paper is to derive this improved bound, replacing Eq. (8), utilizing minimization variational principles for the complex effective permittivity derived by Gibiansky and Cherkaev [9] (that also apply to other problems with complex moduli, such as viscoelasticity [9], and which have later been extended to other non-self-adjoint problems [49], to wave equations in lossy media [50,51], and to scattering problems [52]). These variational principles allow one to use powerful techniques for deriving bounds, namely the variational approach of Hashin and Shtrikman [36] and the translation method, also known as the method of compensated compactness, of Tartar and Murat [10,13,14] and Lurie and Cherkaev [11,12] (see also Refs. [1,53–55]). One advantage of the variational approach, as opposed to the analytic approach of Bergman and Milton, is that it easily extends to multiphase media and to media with anisotropic phases (including polycrystalline media) that have complex permittivity tensors or complex elasticity tensors. Some elementary bounds on the effective complex permittivity tensor and the effective complex elasticity tensor are given in Ref. [49] (see also Sec. 22.6 in Ref. [1]). Some of these bounds have also been conjectured or derived using the analytic approach [56–62] but generally with much greater difficulty. Our analysis is close to that used in Ref. [15] to derive bounds on the effective complex bulk modulus, which has later been extended to bounds on the effective complex shear modulus [63,64] (see also Refs. [65,66]).

The BM bound and our improved bound, like many bounds on effective moduli that involve the volume fractions of the phases (as well as possibly other information), simplify when expressed in terms of their y transforms (see Chaps. 19 and 26 and Secs. 23.6 and 24.10 in Ref. [1] and references therein). Rather than working with bounds on ε_*, one works with bounds on its y transform

$$y_\varepsilon = -f_2\varepsilon_1 - f_1\varepsilon_2 + \frac{f_1f_2(\varepsilon_1-\varepsilon_2)^2}{f_1\varepsilon_1+f_2\varepsilon_2-\varepsilon_*}, \tag{13}$$

in terms of which

$$\varepsilon_* = f_1\varepsilon_1 + f_2\varepsilon_2 - \frac{f_1f_2(\varepsilon_1-\varepsilon_2)^2}{f_2\varepsilon_1+f_1\varepsilon_2+y_\varepsilon}. \tag{14}$$

The BM bounds confine y_ε to a volume-fraction-independent lens-shaped region bounded by the straight line joining $2\varepsilon_1$ and $2\varepsilon_2$, corresponding to the bound (7), and a segment of a circular arc joining $2\varepsilon_1$ and $2\varepsilon_2$ that, when extended, passes through the origin, corresponding to the bound (8). Our improved bound, which replaces this circular arc, is the outermost of two circular arcs joining $2\varepsilon_1$ and $2\varepsilon_2$: one arc when extended passes through $-\varepsilon_1$, while the other arc when extended passes through $-\varepsilon_2$.

Note that while we obtain an improved bound for isotropic composites, our bound also applies to anisotropic composites if we replace the scalar effective permittivity, ε_*, with $\mathrm{Tr}(\boldsymbol{\varepsilon}_*)/3$ or any other effective permittivity of isotropic polycrystals.

II. ON THE OPTIMALITY OF THE SINGLE-RESONANCE BOUND

In the following, we show that the bound (7) is at least almost optimal. First, we derive expressions for the y-transformed effective permittivities of the five known optimal microstructures and discuss corresponding hierarchical laminates. We then show that there are, depending on the volume fraction, at least two or three additional optimal laminates. In the last part of this section, using

numerical calculations, we consider related laminates that come very close to attaining the bound.

The first two of the five microstructures that are known to attain the bound (7) are the two Hashin-Shtrikman coated-sphere assemblages (CS). For phase 1 as the core material, the y-transformed effective permittivity of the assemblage is given by $y_\varepsilon^{\mathrm{CS1}} = 2\varepsilon_2$. For phase 2 as the core material, one obtains $y_\varepsilon^{\mathrm{CS2}} = 2\varepsilon_1$. The third and the fourth optimal microstructure are Schulgasser laminates formed from assemblages of coated cylinders (CC). The effective permittivity of such an assemblage in the directions perpendicular to the cylinder axes is given by

$$\varepsilon_*^{\mathrm{CC1},\perp} = \varepsilon_2 + \frac{2f_1\varepsilon_2(\varepsilon_1-\varepsilon_2)}{2\varepsilon_2 + f_2(\varepsilon_1-\varepsilon_2)}, \tag{15}$$

while parallel to the cylinder axes, one obtains

$$\varepsilon_*^{\mathrm{CC1},\parallel} = f_1\varepsilon_1 + f_2\varepsilon_2. \tag{16}$$

The corresponding Schulgasser laminate has effective permittivity

$$\varepsilon_*^{\mathrm{CC1}} = \frac{1}{3}\left(2\varepsilon_*^{\mathrm{CC1},\perp} + \varepsilon_*^{\mathrm{CC1},\parallel}\right) \tag{17}$$

and its y-transformed effective permittivity is given by

$$y_\varepsilon^{\mathrm{CC1}} = f_1 y_\varepsilon^{\mathrm{CS1}} + f_2\left(\frac{3}{4}y_\varepsilon^{\mathrm{CS1}} + \frac{1}{4}y_\varepsilon^{\mathrm{CS2}}\right). \tag{18}$$

Analogously, one obtains for the phase-interchanged microstructure, i.e., for phase 2 as the core material,

$$y_\varepsilon^{\mathrm{CC2}} = f_2 y_\varepsilon^{\mathrm{CS2}} + f_1\left(\frac{3}{4}y_\varepsilon^{\mathrm{CS2}} + \frac{1}{4}y_\varepsilon^{\mathrm{CS1}}\right). \tag{19}$$

The fifth optimal microstructure, the Schulgasser laminate formed from a rank-1 laminate (L), has effective permittivity

$$\varepsilon_*^{\mathrm{L}} = \frac{1}{3}\left(2\left(f_1\varepsilon_1 + f_2\varepsilon_2\right) + \left(\frac{f_1}{\varepsilon_1} + \frac{f_2}{\varepsilon_2}\right)^{-1}\right) \tag{20}$$

and, therefore,

$$y_\varepsilon^{\mathrm{L}} = f_1 y_\varepsilon^{\mathrm{CS1}} + f_2 y_\varepsilon^{\mathrm{CS2}} = f_1 \times 2\varepsilon_2 + f_2 \times 2\varepsilon_1. \tag{21}$$

This last relation implies that every point on the y-transformed version of the bound (7) is attained by a rank-1 laminate with some volume fraction $f_1 \in [0,1]$. Hence, there can be no tighter bound that is volume fraction independent when expressed in terms of the y-transformed complex permittivity.

It is well known that for each assemblage of coated ellipsoids, there is a hierarchical laminate with the same effective permittivity (see Ref. [14] and Chap. 9 in Ref. [1]). Hierarchical laminates are laminates that are formed in more than one lamination step, i.e., they are laminates of laminates. It is assumed that the length scales of subsequent lamination steps, the number of which is referred to as the rank of the laminate, are sufficiently separated. More precisely, the coated-ellipsoid assemblages correspond to a specific type of hierarchical laminates, so-called coated laminates—first studied by Maxwell [67]—that are formed as follows. In the first lamination step, a laminate is formed from the two pure phases. One of these phases is referred to as the core phase, while the other phase is the so-called coating phase. In all subsequent lamination steps, the laminate obtained in the previous lamination step is laminated with the coating phase. For mutually orthogonal lamination directions and a particular choice of the volume fractions (see Chap. 9 in Ref. [1]), one obtains rank-2 and rank-3 coated laminates equivalent to the Hashin-Shtrikman assemblages of coated cylinders and spheres, respectively. Thus, the five microstructures that are known to attain the bound (7) can equivalently be seen as hierarchical laminates.

Hierarchical laminates are conveniently described using tree structures (see, e.g., Chap. 9 in Ref. [1]). More precisely, every hierarchical laminate can be represented by a tree in which every node has either zero or two children. Nodes of the tree that have zero children, which are commonly referred to as leaves, correspond to one of the pure phases. Each node that is not a leaf, on the other hand, refers to a laminate that is formed from its children and, thus, has a certain lamination direction assigned to it. In the case of three-dimensional orthogonal laminates, there are only three possible lamination directions ($\hat{x}$, $\hat{y}$, and $\hat{z}$). Furthermore, we have to specify the volume fractions used in each lamination step. In our tree representation, we assign these volume fractions to the edges that connect the corresponding node to its children, i.e., the edges of the tree have certain weights. As an example, the tree structures of the laminates corresponding to the coated-cylinder assemblage and the coated-sphere assemblage are shown in Figs. 3(a) and 3(b), respectively.

In order to identify additional microstructures attaining the bound (7), we now consider the class of hierarchical laminates that contains the five known optimal microstructures, i.e., the class of Schulgasser laminates formed from orthogonal laminates that have only one pole. More precisely, we form hierarchical laminates from laminates that are known to attain the bound (or one of the pure phases) in such a way that no additional poles are introduced. The first such hierarchical laminate (LA1) is formed from phase 1 and the laminate corresponding to the coated-cylinder assemblage (with phase 1 as the core phase and phase 2 as the coating phase). It is closely related to the rank-3 coated

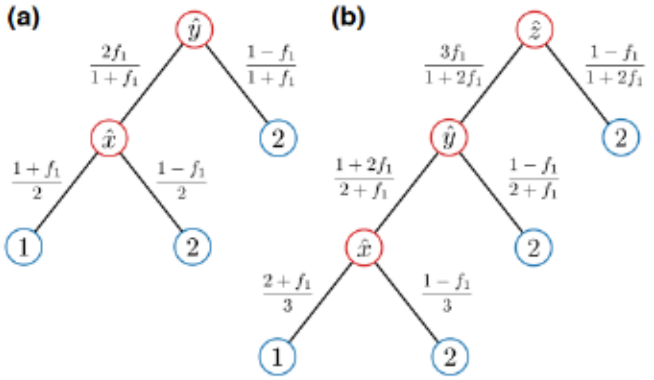

FIG. 3. Tree structures corresponding to hierarchical laminates that have the same effective permittivity as the Hashin-Shtrikman coated-cylinder assemblage (a) and coated-sphere assemblage (b). The blue nodes, i.e., the leaves of the tree, correspond to one of the two pure phases, phase 1 or phase 2, while the red nodes describe a lamination step along one of the three orthogonal lamination directions, $\hat{x}$, $\hat{y}$, or $\hat{z}$. The volume fractions used in the different lamination steps are assigned to the edges of the tree, where f_1 is the volume fraction of phase 1 in the final material. Thus, the volume fractions on the two edges entering each node sum to one.

laminate that corresponds to the coated-sphere assemblage. However, instead of laminating with phase 2, i.e., the coating phase, in the third and last lamination step, we laminate with phase 1. Illustrations of this hierarchical laminate as well as the corresponding tree structure are shown in Fig. 4. As indicated there, we denote the volume fractions used in the different lamination steps by $f^{(i)}$. These volume fractions are uniquely determined by the requirement that the pole that is formed in the last lamination step is identical to the pole of the laminate corresponding to the coated-cylinder assemblage, i.e.,

$$\frac{\varepsilon_2}{\varepsilon_1} = \frac{f_2^{(2)}}{f_2^{(2)} - 2} = \frac{\left(1 - f_2^{(2)}\right)\left(f^{(3)} - 1\right) - f^{(3)}}{\left(1 - f^{(3)}\right) f_2^{(2)}}, \quad (22)$$

where $f_2^{(2)} = 1 - f^{(1)} f^{(2)}$ is the volume fraction of phase 2 in the laminate corresponding to the coated-cylinder assemblage. As the volume fraction of phase 1 in the final laminate is given by

$$f_1 = 1 - f^{(3)} f_2^{(2)}, \quad (23)$$

and as all volume fractions have to lie in the range $[0, 1]$, we can construct this laminate if only if $f_1 \in [1/2, 1]$. Analogously, we can construct the corresponding phase-interchanged hierarchical laminate (LA2) if and only if $f_1 \in [0, 1/2]$. In the final step, in order to obtain isotropic optimal composites, we form Schulgasser laminates from the anisotropic hierarchical laminates LA1 and LA2. The y-transformed effective permittivities of these Schulgasser

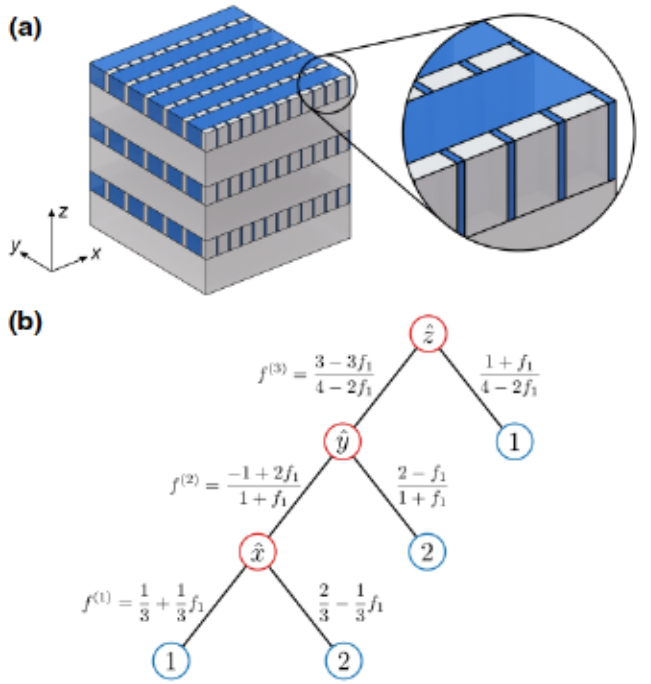

FIG. 4. A schematic illustration (a) and the tree structure (b) of the optimal laminate (LA1) that is formed by laminating the rank-2 laminate corresponding to the coated-cylinder assemblage with phase 1. The volume fractions used in the different lamination steps, $f^{(i)}$, are uniquely determined by the requirement that the structure has only one pole. The Schulgasser laminate formed from the anisotropic material obtained via this lamination scheme, i.e., from the material at the root of the tree, is an optimal isotropic material attaining the bound (7). In (a), phases 1 and 2 are shown in gray and blue, respectively.

laminates are identical and given by the arithmetic mean of the y-transformed permittivities of the two Hashin-Shtrikman coated-sphere assemblages,

$$y_\varepsilon^{\mathrm{LA1}} = y_\varepsilon^{\mathrm{LA2}} = \frac{1}{2}\left(y_\varepsilon^{\mathrm{CS1}} + y_\varepsilon^{\mathrm{CS2}}\right) = \varepsilon_1 + \varepsilon_2, \quad (24)$$

which implies that they attain the bound (7).

In a similar fashion, we can obtain an additional optimal microstructure (LB1) by laminating the hierarchical laminate corresponding to the coated-cylinder assemblage with a rank-1 laminate. The corresponding tree structure is shown in Fig. 5. Again, let $f^{(i)}$ denote the volume fractions used in the different lamination steps. We first require that the pole of the rank-1 laminate is identical to the pole of the laminate corresponding to the coated-cylinder assemblage. With $f_1^{(2)} = f^{(1)} f^{(2)}$ being the volume fraction of phase 2 in the latter laminate, this condition reads

$$\frac{\varepsilon_2}{\varepsilon_1} = \frac{f^{(3)} - 1}{f^{(3)}} = \frac{f_1^{(2)} - 1}{f_1^{(2)} + 1}. \quad (25)$$

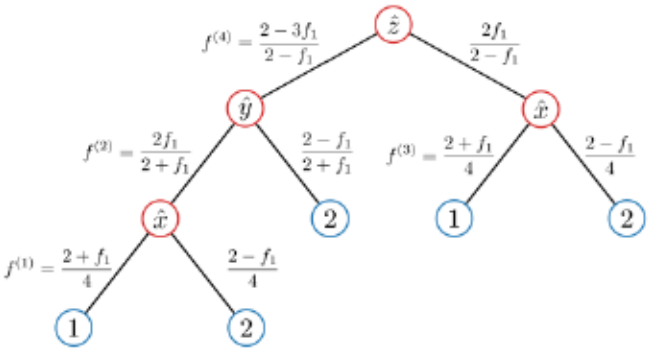

FIG. 5. The tree structure of the optimal laminate (LB1) that is formed by laminating the rank-2 laminate corresponding to the coated-cylinder assemblage with a rank-1 laminate. The Schulgasser laminate made from this material attains the bound (7). As in the case of the laminate shown in Fig. 4, the volume fractions $f^{(i)}$ follow uniquely by requiring that the laminations do not lead to additional poles.

We then require that the pole created in the last lamination step is identical to the pole of the two laminates from which it is formed,

$$\frac{\varepsilon_2}{\varepsilon_1} = \frac{f^{(3)} - 1}{f^{(3)}} = \frac{\left(1 - f^{(4)}\right)\left(f^{(3)} - 1\right) + f^{(3)}}{\left(1 - f^{(4)}\right)\left(f^{(3)} - 1\right) + f^{(3)} - 1}. \quad (26)$$

The volume fraction of phase 1 in the final laminate is given by

$$f_1 = f^{(4)} f_1^{(2)} + \left(1 - f^{(4)}\right) f^{(3)}, \quad (27)$$

which, in combination with the conditions (25) and (26), uniquely determines the volume fractions $f^{(i)}$. As these volume fractions have to lie in the range $[0, 1]$, the laminate LB1 can be constructed if and only if $f_1 \in [0, 2/3]$. The y-transformed effective permittivity of the corresponding Schulgasser laminate is given by

$$y_\varepsilon^{\mathrm{LB1}} = f^{(4)} y_\varepsilon^{\mathrm{CC1}} + \left(1 - f^{(4)}\right) y_\varepsilon^{\mathrm{L}}. \quad (28)$$

Similarly, we can find a corresponding laminate with interchanged phases (LB2), with

$$y_\varepsilon^{\mathrm{LB2}} = f^{(4)} y_\varepsilon^{\mathrm{CC2}} + \left(1 - f^{(4)}\right) y_\varepsilon^{\mathrm{L}}, \quad (29)$$

if and only if $f_1 \in [1/3, 0]$. As these points, $y_\varepsilon^{\mathrm{LB1}}$ and $y_\varepsilon^{\mathrm{LB2}}$, lie on the straight line joining $2\varepsilon_1$ and $2\varepsilon_2$, the Schulgasser laminates formed from these laminates attain the bound (7).

Hence, in summary, we obtain three additional microstructures attaining the bound if $f_1 \in (1/3, 2/3)$ with $f_1 \neq 1/2$ and two additional microstructures otherwise. While it remains presently unclear whether this strategy succeeds for every permittivity on the bound, using numerical calculations, one can interpolate between the known optimal laminates in such a way that the resulting laminates, which in general have more than a single pole, come very close to the bound. In order to do so, we choose two of the known optimal laminates (CS1, CS2, CC1, CC2, and L), which we refer to as laminates A and B, and laminate them along one of the three axes in proportions f and $1 - f$. If f_1^{A} and f_1^{B} are the volume fractions of phase 1 in the laminates A and B, respectively, the volume fraction of phase 1 in the resulting material is given by

$$f_1 = f\, f_1^{\mathrm{A}} + (1 - f) f_1^{\mathrm{B}}. \quad (30)$$

As, in general, this laminate is not isotropic, we form a Schulgasser laminate in the final step. We then repeat this process for all three axes and for all possible pairwise combinations of the laminates CS1, CS2, CC1, CC2, and L and a large number of combinations of f_1^{A} and f_1^{B} while varying f such that f_1 is kept fixed. We calculate the corresponding effective complex permittivities numerically. The results for different sets of parameters are shown in Fig. 6. Both close to and far off resonance, the laminates closely approach the bound (7), which demonstrates that, for all practical purposes, it can be considered to be optimal. Moreover, the laminates fill the region between the bounds almost completely except for a gap close to the doubly-coated-sphere assemblage, which is especially pronounced in Fig. 6(d). This gap can be readily filled by, e.g., forming a laminate with the doubly-coated-sphere assemblage.

III. AN OPTIMAL BOUND ON THE EFFECTIVE PERMITTIVITY

We now derive our improved bound on the isotropic effective electric permittivity that corresponds to the doubly-coated-sphere assemblage. In the first step, following Cherkaev and Gibiansky [9] (see also Sec. 11.5 in Ref. [1]), we rewrite the constitutive relation in terms of the real (primed) and imaginary (double-primed) parts of the fields,

$$\begin{pmatrix} \mathbf{e}'' \\ \mathbf{d}'' \end{pmatrix} = \mathbf{L} \begin{pmatrix} -\mathbf{d}' \\ \mathbf{e}' \end{pmatrix}, \quad (31)$$

with $\mathbf{L} = \begin{pmatrix} (\boldsymbol{\varepsilon}'')^{-1} & (\boldsymbol{\varepsilon}'')^{-1}\boldsymbol{\varepsilon}' \\ \boldsymbol{\varepsilon}'(\boldsymbol{\varepsilon}'')^{-1} & \boldsymbol{\varepsilon}'(\boldsymbol{\varepsilon}'')^{-1}\boldsymbol{\varepsilon}' + \boldsymbol{\varepsilon}'' \end{pmatrix}$ being symmetric and positive definite. Now, we can recast the problem of finding the effective permittivity tensor as the following minimization variational principle (see also Ref. [9]):

$$\begin{pmatrix} -\mathbf{d}_0' \\ \mathbf{e}_0' \end{pmatrix} \cdot \mathbf{L}_* \begin{pmatrix} -\mathbf{d}_0' \\ \mathbf{e}_0' \end{pmatrix} \quad (32)$$
$$= \min \left\{ \left\langle \begin{pmatrix} -\mathbf{d}' \\ \mathbf{e}' \end{pmatrix} \cdot \mathbf{L} \begin{pmatrix} -\mathbf{d}' \\ \mathbf{e}' \end{pmatrix} \right\rangle \middle| \begin{matrix} \langle \mathbf{d}' \rangle = \mathbf{d}_0', \ \nabla \cdot \mathbf{d}' = 0 \\ \langle \mathbf{e}' \rangle = \mathbf{e}_0', \ \nabla \times \mathbf{e}' = 0 \end{matrix} \right\}.$$

Using a constant trial field, one immediately obtains the arithmetic mean bound $\mathbf{L}_* \leq \langle \mathbf{L} \rangle$, while the corresponding dual variational principle leads to the harmonic mean

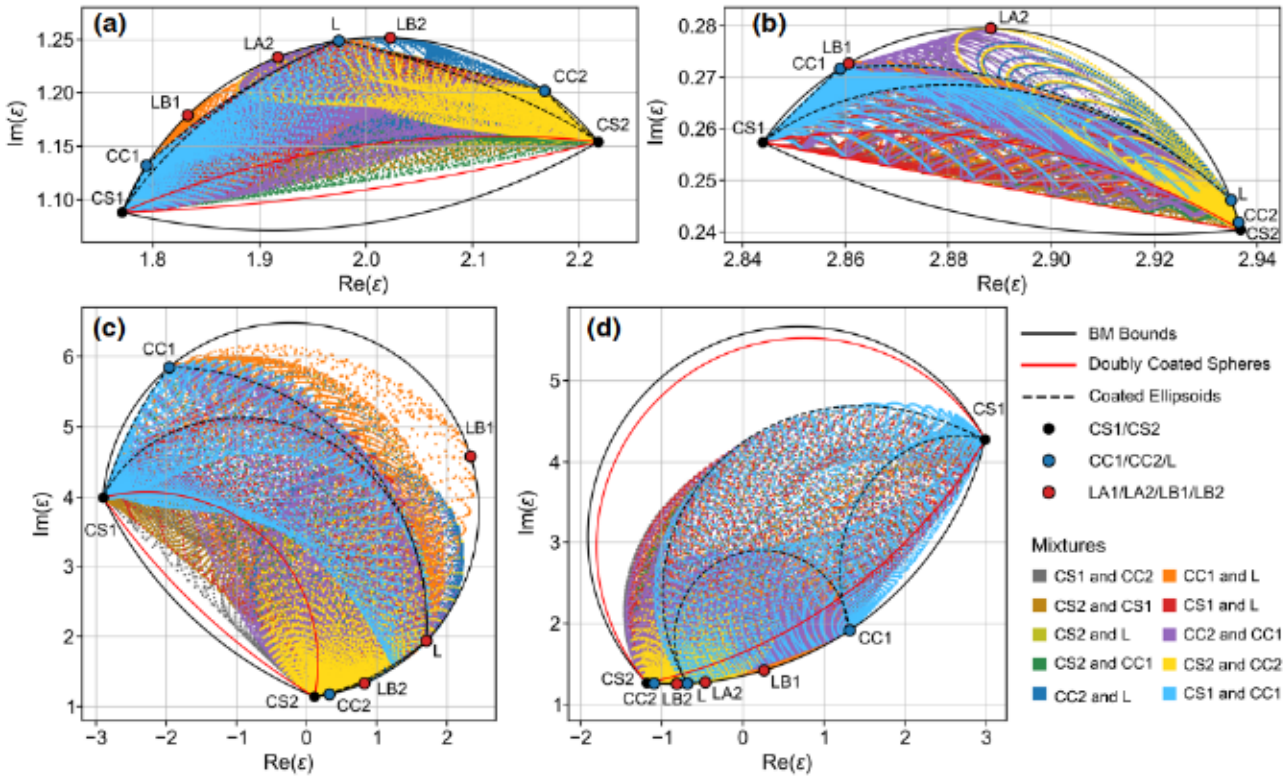

FIG. 6. Numerical calculations of the effective complex permittivities (small squares) of Schulgasser laminates of microstructures formed by pairwise laminating the previously identified optimal laminates, CS1, CS2, CC1, CC2, and L. The different colors correspond to the different combinations of optimal laminates. The laminates formed in this way closely approach the BM bound corresponding to single-resonance structures, which is attained by the Hashin-Shtrikman coated-sphere assemblages (black dots), the optimal microstructures previously identified by Milton (blue dots), and the hierarchical laminates described above (red dots). The boundary of the region attained by Schulgasser laminates of assemblages of coated ellipsoids is shown for reference (dashed curve). The two red curves correspond to assemblages of doubly coated spheres. In Sec. III of this paper, we show that the outermost of these two curves is actually a bound. Note that the density of points in these plots in no way signifies the probability of obtaining such permittivities in experiments. The parameters are chosen as follows. In (a) and (b), corresponding to the situation far off resonance, the constituent permittivities are $\varepsilon_1 = 0.2 + 1.76i$ and $\varepsilon_2 = 3 + 0.1i$, respectively. While in (a) a moderate volume fraction of $f_1 = 0.4$ is chosen, (b) corresponds to the dilute limit, $f_1 = 0.05$. In both cases, for these specific choices of parameters, one of the hierarchical laminates identified here attains the largest possible imaginary part, i.e., it shows the strongest possible absorption. The parameters in (c) and (d) are $\varepsilon_1 = -4.6 + 2.4i$, $\varepsilon_2 = 2.5 + 0.1i$, and $f_1 = 0.5$ and $\varepsilon_1 = -4.6 + 2.4i$, $\varepsilon_2 = 2.5 + 0.1i$, and $f_1 = 0.4$, respectively.

bound $\mathbf{L}_*^{-1} \leq \langle \mathbf{L}^{-1} \rangle$. Note that these two bounds are equivalent in the sense that they lead to the same bounds on the effective permittivity tensor [9].

Before applying the translation method, we first embed the variational problem (32) in a variational problem involving a tensor of higher rank [14,43,68] (see also Sec. 24.8 in Ref. [1]). Instead of working with the rank-2 tensor $\mathbf{L}$, we consider a corresponding rank-4 tensor, $\boldsymbol{\mathcal{L}}$, that comprises several copies of $\mathbf{L}$. Intuitively speaking, this approach allows us to simultaneously probe the composite material along different directions.

As the microscopic electric field, $\mathbf{e}(\mathbf{x})$, and the microscopic electric displacement field, $\mathbf{d}(\mathbf{x})$, depend linearly on the macroscopic electric field, $\langle \mathbf{e} \rangle$, we can write

$$\mathbf{e}(\mathbf{x}) = \mathbf{E}(\mathbf{x})\langle \mathbf{e} \rangle \quad \text{and} \quad \mathbf{d}(\mathbf{x}) = \mathbf{D}(\mathbf{x})\langle \mathbf{e} \rangle, \tag{33}$$

thereby introducing the rank-2 tensor fields $\mathbf{E}(\mathbf{x})$ and $\mathbf{D}(\mathbf{x})$, which, as opposed to a single solution of the quasistatic Eq. (1), fully characterize the composite material. The corresponding microscopic version of the constitutive law takes the form

$$\mathbf{D} = \boldsymbol{\mathcal{E}} : \mathbf{E}, \tag{34}$$

where ":" denotes a contraction with respect to two indices, i.e.,

$$D_{ij} = \mathcal{E}_{ijkl} E_{kl}, \tag{35}$$

and $\boldsymbol{\mathcal{E}}$ is a rank-4 tensor with components

$$\mathcal{E}_{ijkl} = \varepsilon_{ik}\delta_{jl} \quad \text{with } i,j,k,l \in \{1,2,3\}. \tag{36}$$

The macroscopic version of the constitutive law, which defines the corresponding effective tensor, is given by

$$\langle \mathbf{D} \rangle = \boldsymbol{\mathcal{E}}_* : \langle \mathbf{E} \rangle. \tag{37}$$

Using $\langle \mathbf{E} \rangle = \mathbf{I}$ and considering an isotropic composite, Eq. (37) reduces to $\langle \mathbf{D} \rangle = \varepsilon_* \mathbf{I}$, where ε_* is the scalar effective permittivity. As the fields $\mathbf{e}$ and $\mathbf{d}$ are curl and divergence free, respectively, we can find corresponding differential constraints on $\mathbf{E}$ and $\mathbf{D}$:

$$\epsilon_{ijk} \partial_j E_{kl} = 0 \quad \text{and} \quad \partial_i D_{ij} = 0. \tag{38}$$

As in the rank-2 case, cf. Eq. (31), we can rewrite the constitutive law in terms of the real and imaginary parts:

$$\begin{pmatrix} \mathbf{E}'' \\ \mathbf{D}'' \end{pmatrix} = \boldsymbol{\mathcal{L}} : \begin{pmatrix} -\mathbf{D}' \\ \mathbf{E}' \end{pmatrix}, \tag{39}$$

with

$$\boldsymbol{\mathcal{L}} = \begin{pmatrix} (\boldsymbol{\mathcal{E}}'')^{-1} & (\boldsymbol{\mathcal{E}}'')^{-1} \boldsymbol{\mathcal{E}}' \\ \boldsymbol{\mathcal{E}}' (\boldsymbol{\mathcal{E}}'')^{-1} & \boldsymbol{\mathcal{E}}' (\boldsymbol{\mathcal{E}}'')^{-1} \boldsymbol{\mathcal{E}}' + \boldsymbol{\mathcal{E}}'' \end{pmatrix}, \tag{40}$$

where we have introduced the rank-4 tensor $\boldsymbol{\mathcal{L}}$. The components of this tensor are related to the components of the corresponding rank-2 tensor as follows:

$$\mathcal{L}_{ijkl} = L_{ik} \delta_{jl} \quad \text{with } j, l \in \{1, 2, 3\}, \;\; i, k \in \{1, \ldots, 6\}. \tag{41}$$

We now consider a material with translated properties,

$$\widetilde{\boldsymbol{\mathcal{L}}}(\mathbf{x}) = \boldsymbol{\mathcal{L}}(\mathbf{x}) - \mathbf{T}, \tag{42}$$

satisfying the following two conditions (see, e.g., Ref. [68, 69] and Chap. 24 in Ref. [1]):

(i) The translated tensor is positive semidefinite, i.e.,

$$\boldsymbol{\mathcal{L}}(\mathbf{x}) - \mathbf{T} \geq 0, \tag{43}$$

which, as we are considering a two-phase medium, simplifies to

$$\boldsymbol{\mathcal{L}}_1 - \mathbf{T} \geq 0 \quad \text{and} \quad \boldsymbol{\mathcal{L}}_2 - \mathbf{T} \geq 0. \tag{44}$$

(ii) The translation, $\mathbf{T}$, is quasiconvex, i.e.,

$$\langle \mathbf{F} : \mathbf{T} : \mathbf{F} \rangle - \langle \mathbf{F} \rangle : \mathbf{T} : \langle \mathbf{F} \rangle \geq 0 \tag{45}$$

for all $\mathbf{F} = (-\mathbf{D}', \mathbf{E}')^{\mathsf{T}}$, with the periodic fields $\mathbf{D}'$ and $\mathbf{E}'$ subject to the usual differential constraints.

Note that if Eq. (45) holds as an equality, $\mathbf{T}$ is said to be a null Lagrangian or, more precisely, the quadratic form associated with $\mathbf{T}$ is a null Lagrangian.

Condition (i) allows us to apply the harmonic mean bound to the translated material,

$$\widetilde{\boldsymbol{\mathcal{L}}}_*^{-1} \leq \langle \widetilde{\boldsymbol{\mathcal{L}}}^{-1} \rangle, \tag{46}$$

and condition (ii) implies that

$$\widetilde{\boldsymbol{\mathcal{L}}}_* \leq \boldsymbol{\mathcal{L}}_* - \mathbf{T}. \tag{47}$$

In combination, we obtain the so-called translation bound:

$$\begin{aligned} (\boldsymbol{\mathcal{L}}_* - \mathbf{T})^{-1} &\leq \langle (\boldsymbol{\mathcal{L}} - \mathbf{T})^{-1} \rangle \\ &= f_1 (\boldsymbol{\mathcal{L}}_1 - \mathbf{T})^{-1} + f_2 (\boldsymbol{\mathcal{L}}_2 - \mathbf{T})^{-1}. \end{aligned} \tag{48}$$

Analogous to the y transform of the scalar effective parameters given in Eq. (13), we can introduce the y transform of the effective tensor $\boldsymbol{\mathcal{L}}_*$,

$$\begin{aligned} \mathbf{Y} = &-f_1 \boldsymbol{\mathcal{L}}_2 - f_2 \boldsymbol{\mathcal{L}}_1 + f_1 f_2 (\boldsymbol{\mathcal{L}}_1 - \boldsymbol{\mathcal{L}}_2) \\ &\cdot (f_1 \boldsymbol{\mathcal{L}}_1 + f_2 \boldsymbol{\mathcal{L}}_2 - \boldsymbol{\mathcal{L}}_*)^{-1} \cdot (\boldsymbol{\mathcal{L}}_1 - \boldsymbol{\mathcal{L}}_2), \end{aligned} \tag{49}$$

in terms of which the bound takes the particularly simple form

$$\mathbf{Y} + \mathbf{T} \geq 0. \tag{50}$$

While in principle, we could consider any arbitrary translation satisfying the aforementioned conditions, it has been shown that isotropic translations, reflecting the symmetry of the problem, are most well suited [68]. We start by noting that any arbitrary isotropic rank-four tensor can be written as

$$\begin{aligned} A_{ijkl}(\lambda_1, \lambda_2, \lambda_3) = &\frac{\lambda_1}{3} \delta_{ij} \delta_{kl} \\ &+ \frac{\lambda_2}{2} \left(\delta_{ik} \delta_{jl} + \delta_{il} \delta_{jk} - \frac{2}{3} \delta_{ij} \delta_{kl} \right) + \frac{\lambda_3}{2} \left(\delta_{ik} \delta_{jl} - \delta_{il} \delta_{jk} \right), \end{aligned} \tag{51}$$

where the three terms correspond to projections of an arbitrary rank-2 tensor onto the subspaces of tensors proportional to the indentity tensor, trace-free symmetric tensors, and antisymmetric tensors. We refer to these three terms as the bulk-modulus, shear-modulus, and antisymmetrization terms, since in elasticity the coefficients λ_1 and λ_2 correspond to the bulk and shear modulus, respectively, while λ_3 has no counterpart as the elasticity tensor is symmetric with respect to permutations of the first two (as well as the last two) indices. In the following, we encounter tensors of

the form

$$\begin{pmatrix} \mathbf{A}(\lambda_1,\lambda_2,\lambda_3) & \mathbf{A}(\lambda_4,\lambda_5,\lambda_6) \\ \mathbf{A}(\lambda_4,\lambda_5,\lambda_6) & \mathbf{A}(\lambda_7,\lambda_8,\lambda_9) \end{pmatrix}. \tag{52}$$

We use the fact that such a tensor is positive semidefinite if and only if the three matrices

$$\begin{pmatrix} \lambda_1 & \lambda_4 \\ \lambda_4 & \lambda_7 \end{pmatrix}, \quad \begin{pmatrix} \lambda_2 & \lambda_5 \\ \lambda_5 & \lambda_8 \end{pmatrix}, \quad \text{and} \quad \begin{pmatrix} \lambda_3 & \lambda_6 \\ \lambda_6 & \lambda_9 \end{pmatrix} \tag{53}$$

are positive semidefinite. We now choose the translation as

$$\mathbf{T}(t_1,t_2,t_3) = \begin{pmatrix} \mathbf{A}(-t_1,2t_1,0) & \mathbf{A}(-t_3,-t_3,-t_3) \\ \mathbf{A}(-t_3,-t_3,-t_3) & \mathbf{A}(-2t_2,t_2,-t_2) \end{pmatrix}, \tag{54}$$

for $t_1 \geq 0$ and t_2 and t_3 arbitrary.

In order to show that such a translation is quasiconvex, as shown by Tartar [14,70] and Murat and Tartar [13] (see also Sec. 24.3 in Ref. [1]), and following the analogous discussion in Ref. [15], it turns out to be useful to consider the Fourier series of the real parts of the fields,

$$\mathbf{E}' = \langle \mathbf{E}' \rangle + \sum_{k\neq 0} e^{-i\mathbf{k}\cdot\mathbf{x}} \mathbf{E}_\mathbf{k}, \tag{55}$$

and

$$\mathbf{D}' = \langle \mathbf{D}' \rangle + \sum_{k\neq 0} e^{-i\mathbf{k}\cdot\mathbf{x}} \mathbf{D}_\mathbf{k}. \tag{56}$$

Since $\mathbf{E}$ and $\mathbf{D}$ are curl and divergence free, respectively, we obtain the following constraints on the Fourier coefficients:

$$\mathbf{k}\times\mathbf{E}_\mathbf{k} = 0 \quad \text{and} \quad \mathbf{k}\cdot\mathbf{D}_\mathbf{k} = 0. \tag{57}$$

Using Plancherel's identity, one finds that, in order to prove the quasiconvexity of the translation, it suffices to show that

$$\sum_{\mathbf{k}\neq 0} \overline{\mathbf{D}}_\mathbf{k} : \mathbf{A}(-t_1,2t_1,0) : \mathbf{D}_\mathbf{k} \geq 0, \tag{58}$$

$$\sum_{\mathbf{k}\neq 0} \overline{\mathbf{E}}_\mathbf{k} : \mathbf{A}(-2t_2,t_2,-t_2) : \mathbf{E}_\mathbf{k} = 0, \tag{59}$$

$$\sum_{\mathbf{k}\neq 0} \overline{\mathbf{D}}_\mathbf{k} : \mathbf{A}(-t_3,-t_3,-t_3) : \mathbf{E}_\mathbf{k} = 0, \tag{60}$$

where $\overline{\mathbf{E}}_\mathbf{k}$ denotes the complex conjugate of $\mathbf{E}_\mathbf{k}$. Note that we choose $\mathbf{A}(-2t_2,t_2,-t_2)$ and $\mathbf{A}(-t_3,-t_3,-t_3)$ to be null Lagrangians (with respect to the appropriate subspaces) rather than merely satisfying the condition of quasiconvexity. As we are considering isotropic tensors, it is sufficient to consider a single choice of $\mathbf{k}$. For example, for $\mathbf{k} = (1,0,0)^\intercal$, the constraints (57) imply that the fields have the form

$$\mathbf{D}_\mathbf{k} = \begin{pmatrix} 0 & 0 & 0 \\ D_{21} & D_{22} & D_{23} \\ D_{31} & D_{32} & D_{33} \end{pmatrix} \quad \text{and} \quad \mathbf{E}_\mathbf{k} = \begin{pmatrix} E_{11} & E_{12} & E_{13} \\ 0 & 0 & 0 \\ 0 & 0 & 0 \end{pmatrix} \tag{61}$$

and it becomes straightforward to show that the inequalities (58)–(60) hold.

Having established that a translation of the form given in Eq. (54) is quasiconvex, we can now return to the translation bound. Introducing the y transform of the effective tensor $\boldsymbol{\mathcal{E}}_*$,

$$\begin{aligned} \boldsymbol{\mathcal{Y}} = &-f_1\boldsymbol{\mathcal{E}}_2 - f_2\boldsymbol{\mathcal{E}}_1 \\ &+ f_1 f_2 (\boldsymbol{\mathcal{E}}_1 - \boldsymbol{\mathcal{E}}_2)\cdot(f_1\boldsymbol{\mathcal{E}}_1 + f_2\boldsymbol{\mathcal{E}}_2 - \boldsymbol{\mathcal{E}}_*)^{-1}\cdot(\boldsymbol{\mathcal{E}}_1 - \boldsymbol{\mathcal{E}}_2), \end{aligned} \tag{62}$$

we can write (see, e.g., Ref. [15])

$$\mathbf{Y} = \begin{pmatrix} (\boldsymbol{\mathcal{Y}}'')^{-1} & -(\boldsymbol{\mathcal{Y}}'')^{-1}\boldsymbol{\mathcal{Y}}' \\ -\boldsymbol{\mathcal{Y}}'(\boldsymbol{\mathcal{Y}}'')^{-1} & \boldsymbol{\mathcal{Y}}'(\boldsymbol{\mathcal{Y}}'')^{-1}\boldsymbol{\mathcal{Y}}' + \boldsymbol{\mathcal{Y}}'' \end{pmatrix}. \tag{63}$$

Restricting ourselves to isotropic effective permittivities,

$$\boldsymbol{\mathcal{Y}} = y_\varepsilon \mathbf{A}(1,1,1), \tag{64}$$

we then obtain

$$\mathbf{Y} = \begin{pmatrix} (y_\varepsilon'')^{-1}\mathbf{A}(1,1,1) & -(y_\varepsilon'')^{-1}y_\varepsilon'\mathbf{A}(1,1,1) \\ -(y_\varepsilon'')^{-1}y_\varepsilon'\mathbf{A}(1,1,1) & ((y_\varepsilon'')^{-1}(y_\varepsilon')^2 + y_\varepsilon'')\mathbf{A}(1,1,1) \end{pmatrix}. \tag{65}$$

Using the decomposition into the bulk-modulus, shear-modulus, and antisymmetrization terms, it becomes clear that the translation bound reduces to the three conditions

$$\begin{pmatrix} (y_\varepsilon'')^{-1} - t_1 & -(y_\varepsilon'')^{-1}y_\varepsilon' - t_3 \\ -(y_\varepsilon'')^{-1}y_\varepsilon' - t_3 & (y_\varepsilon'')^{-1}(y_\varepsilon')^2 + y_\varepsilon'' - 2t_2 \end{pmatrix} \geq 0, \tag{66}$$

$$\begin{pmatrix} (y_\varepsilon'')^{-1} + 2t_1 & -(y_\varepsilon'')^{-1}y_\varepsilon' - t_3 \\ -(y_\varepsilon'')^{-1}y_\varepsilon' - t_3 & (y_\varepsilon'')^{-1}(y_\varepsilon')^2 + y_\varepsilon'' + t_2 \end{pmatrix} \geq 0, \tag{67}$$

$$\begin{pmatrix} (y_\varepsilon'')^{-1} & -(y_\varepsilon'')^{-1}y_\varepsilon' - t_3 \\ -(y_\varepsilon'')^{-1}y_\varepsilon' - t_3 & (y_\varepsilon'')^{-1}(y_\varepsilon')^2 + y_\varepsilon'' - t_2 \end{pmatrix} \geq 0, \tag{68}$$

which imply that the corresponding determinants are nonnegative. Thus, we obtain from the first of these conditions,

Eq. (66),

$$\frac{t_1}{y_\varepsilon''}\left((y_\varepsilon'-y_c')^2+(y_\varepsilon''-y_c'')^2-R^2\right)\le 0, \tag{69}$$

where we have introduced the parameters

$$y_c'=-\frac{t_3}{t_1},\quad y_c''=\frac{1+2t_1t_2-t_3^2}{2t_1},$$
$$R=\left|\frac{1-2t_1t_2+t_3^2}{2t_1}\right|. \tag{70}$$

Hence, the y-transformed effective permittivity has to lie inside of or on a circle with center (y_c', y_c'') and radius R. Choosing different translations, i.e., different values of t_1, t_2, and t_3, corresponds to moving and scaling the circle in the complex plane. In contrast to the complex bulk modulus case [15], the circle may or may not contain the origin, as

$$(y_c')^2+(y_c'')^2-R^2=2\frac{t_2}{t_1} \tag{71}$$

is not necessarily non-negative. As shown below, the first condition leads to bounds that constrain the y-transformed effective permittivity to a region in the complex plane that is bounded by a circular arc and a straight line. As the circular arc turns out to correspond to the doubly-coated-sphere assemblage and the straight line corresponds to the bound (7), which is the tightest possible bound that is volume fraction independent in the y plane, the second and third conditions cannot provide any additional information and may be disregarded.

We now identify the restrictions on the parameters y_c', y_c'', and R, i.e., on the choice of circles bounding the y-transformed effective permittivity, imposed by the condition that the translated tensor is positive semidefinite, i.e., by Eq. (43). Using the fact that the permittivity tensors of the two phases are isotropic,

$$\boldsymbol{\mathcal{E}}_i=\varepsilon_i\mathbf{A}(1,1,1)\quad \text{for } i\in\{1,2\}, \tag{72}$$

we find that

$$\boldsymbol{\mathcal{L}}_i=\begin{pmatrix}(\varepsilon_i'')^{-1}\mathbf{A}(1,1,1) & (\varepsilon_i'')^{-1}\varepsilon_i'\mathbf{A}(1,1,1)\\ (\varepsilon_i'')^{-1}\varepsilon_i'\mathbf{A}(1,1,1) & ((\varepsilon_i'')^{-1}(\varepsilon_i')^2+\varepsilon_i'')\mathbf{A}(1,1,1)\end{pmatrix}. \tag{73}$$

Again using the decomposition into the bulk-modulus, shear-modulus, and antisymmetrization terms, we find that the positive semidefiniteness of the translated tensor is equivalent to the three constraints

$$\begin{pmatrix}(\varepsilon_i'')^{-1}+t_1 & (\varepsilon_i'')^{-1}\varepsilon_i'+t_3\\ (\varepsilon_i'')^{-1}\varepsilon_i'+t_3 & (\varepsilon_i'')^{-1}(\varepsilon_i')^2+\varepsilon_i''+2t_2\end{pmatrix}\ge 0, \tag{74}$$

$$\begin{pmatrix}(\varepsilon_i'')^{-1}-2t_1 & (\varepsilon_i'')^{-1}\varepsilon_i'+t_3\\ (\varepsilon_i'')^{-1}\varepsilon_i'+t_3 & (\varepsilon_i'')^{-1}(\varepsilon_i')^2+\varepsilon_i''-t_2\end{pmatrix}\ge 0, \tag{75}$$

$$\begin{pmatrix}(\varepsilon_i'')^{-1} & (\varepsilon_i'')^{-1}\varepsilon_i'+t_3\\ (\varepsilon_i'')^{-1}\varepsilon_i'+t_3 & (\varepsilon_i'')^{-1}(\varepsilon_i')^2+\varepsilon_i''+t_2\end{pmatrix}\ge 0, \tag{76}$$

which imply that the corresponding determinants are non-negative. Evaluating the first two determinants gives

$$(y_c'+\varepsilon_i')^2+(y_c''+\varepsilon_i'')^2\ge R^2 \tag{77}$$

and

$$(y_c'-2\varepsilon_i')^2+(y_c''-2\varepsilon_i'')^2\le R^2. \tag{78}$$

By considering the remaining principal minors, i.e., the diagonal elements, it can be shown that Eqs. (77) and (78) are not only necessary but also sufficient for the first two constraints, Eqs. (74) and (75). Furthermore, the third constraint, Eq. (76), can be discarded, as it can be written as a weighted arithmetic mean of the other two constraints.

Hence, the restriction to positive-semidefinite translated tensors corresponds to choosing the parameters of the translation such that $2\varepsilon_1$ and $2\varepsilon_2$ do not lie outside of the circle and $-\varepsilon_1$ and $-\varepsilon_2$ do not lie inside of the circle. The extremal translations consistent with this restriction correspond to a generalized circle, the halfspace bounded by the straight line between $2\varepsilon_1$ and $2\varepsilon_2$ that does not contain $-\varepsilon_1$ and $-\varepsilon_2$, and one of the two circles passing through $2\varepsilon_1$, $2\varepsilon_2$, and $-\varepsilon_1$ or $-\varepsilon_2$.

Thus, we find that, as illustrated in Fig. 7, the y-transformed effective complex electric permittivity is bounded by the straight line joining $2\varepsilon_1$ and $2\varepsilon_2$ on one side and the outermost of the two circular arcs passing through $2\varepsilon_1$, $2\varepsilon_2$ and $-\varepsilon_1$ or $-\varepsilon_2$ on the other side. While the former bound, which is the one given in Eq. (7), has been previously derived using the analytic method, the latter bound is tighter than any previously identified bound and even turns out to be optimal, as it corresponds to assemblages of doubly coated spheres. The effective permittivity of such an assemblage (see, e.g., Sec. 7.2 in Ref. [1] for a detailed discussion), with phase 1 in the core and the outer shell and phase 2 in the inner shell, is given by

$$y_\varepsilon^{\mathrm{DCS1}}=2\varepsilon_1\frac{3p\varepsilon_2+(1-p)(\varepsilon_1+2\varepsilon_2)}{3p\varepsilon_1+(1-p)(\varepsilon_1+2\varepsilon_2)}, \tag{79}$$

where the volume fractions of the core, the inner shell, and the outer shell are pf_1, $1-f_1$, and $(1-p)f_1$, respectively. Clearly, this equation corresponds to a circular arc passing through $2\varepsilon_1$, $2\varepsilon_2$, and $-\varepsilon_1$. For the phase-interchanged case, i.e., phase 2 in the core and the outer shell and phase

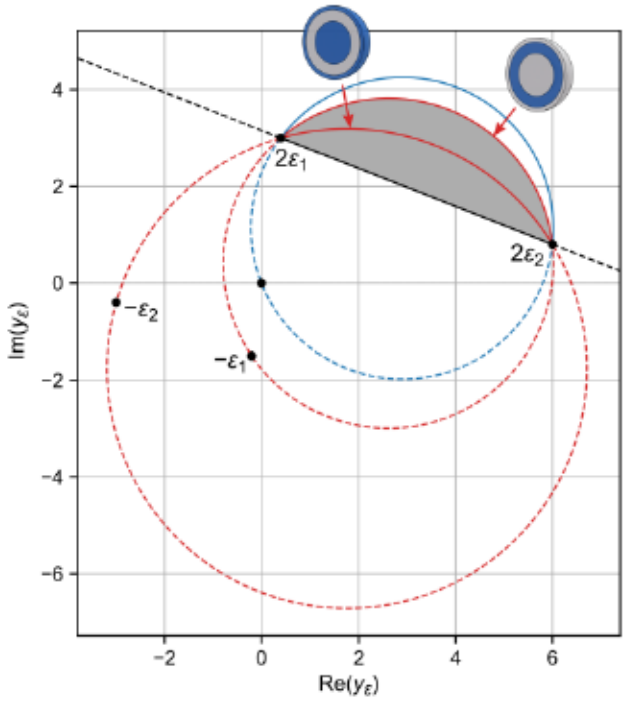

FIG. 7. An illustration of the bounds on the y-transformed effective electric permittivity. The analytic bounds by Bergman and Milton correspond to the straight black line joining $2\varepsilon_1$ and $2\varepsilon_2$ and the blue circular arc passing through $2\varepsilon_1$, $2\varepsilon_2$, and the origin. Using variational methods, we find that y-transformed effective electric permittivity is confined to the gray-shaded region, i.e., the region that is additionally bounded by the outermost of the two red circular arcs passing through $2\varepsilon_1$, $2\varepsilon_2$, and $-\varepsilon_1$ or $-\varepsilon_2$, which correspond to Hashin-Shtrikman assemblages of doubly coated spheres. The parameters are $\varepsilon_1 = 0.2 + 1.5i$ and $\varepsilon_2 = 3 + 0.4i$.

1 in the inner shell, one obtains

$$y_\varepsilon^{\mathrm{DCS2}} = 2\varepsilon_2 \frac{3p\varepsilon_1 + (1-p)(\varepsilon_2 + 2\varepsilon_1)}{3p\varepsilon_2 + (1-p)(\varepsilon_2 + 2\varepsilon_1)}, \tag{80}$$

which corresponds to a circular arc passing through $2\varepsilon_1$, $2\varepsilon_2$, and $-\varepsilon_2$. Here, the volume fractions of the core, the inner shell, and the outer shell are $p(1-f_1)$, f_1, and $(1-p)(1-f_1)$, respectively.

IV. RELATION TO BOUNDS ON THE COMPLEX POLARIZABILITY

As shown in Ref. [71], bounds on the effective complex permittivity for small values of f_1 directly lead to bounds on the orientation averaged complex polarizability of an inclusion (or set of inclusions) having permittivity ε_1 embedded in a medium with permittivity ε_2. Independently, Miller *et al.* [72] have derived explicit bounds on the imaginary part of the polarizability (which describes the absorption of electromagnetic radiation by a cloud of small particles, each much smaller than the wavelength) and subsequently, in Ref. [52], explicit bounds have been obtained on the complex polarizabilty (not just its imaginary part) by taking the dilute limit $f_1 \to 0$ in the BM bounds, keeping the leading term in f_1. It is important to remark that the elementary arguments of Ref. [73] and its recent generalizations incorporating size-dependent radiation effects [74–76] lead to useful bounds that are valid at any wavelength and are not necessarily large compared to the particle size. Our improved bound naturally also applies when the volume fraction f_1 is small and thus produces a tighter and optimal bound on the complex polarizability.

Consider, in the quasistatic regime, a dilute suspension of randomly oriented identical particles in vacuum or air. The effective relative permittivity of such a cloud of particles is given by

$$\boldsymbol{\varepsilon}_* \approx 1 + f_1 \frac{\mathrm{Tr}(\boldsymbol{\alpha})}{3V}, \tag{81}$$

where $\mathrm{Tr}(\boldsymbol{\alpha})/3$ and V are the angle-averaged polarizability tensor and the volume of each of the particles. Then, it follows from the bound (7) and our improved bound corresponding to the doubly-coated-sphere assemblage that the orientation-averaged polarizability per unit volume, $\mathrm{Tr}(\boldsymbol{\alpha})/(3V)$, is bounded by the circular arc

$$\alpha^{\mathrm{BM}}(u) = \chi_1 - \frac{\chi_1^2}{1 + \chi_1 + 2(u\chi_1 + 1)} \tag{82}$$

and the outermost of the straight line-segment

$$\alpha^{\mathrm{DCS1}}(u) = \frac{3\chi_1}{\chi_1 + 3} + \frac{2u\chi_1^3}{3(\chi_1 + 1)(\chi_1 + 3)} \tag{83}$$

and the circular arc

$$\alpha^{\mathrm{DCS2}}(u) = \frac{3\chi_1(3 + 2\chi_1)}{9(\chi_1 + 1) + 2u\chi_1^2}, \tag{84}$$

where χ_1 is the electric susceptibility of the constituent material of the particles and $u \in [0, 1]$. This result improves on the bounds derived in Ref. [52] that follow from the BM bounds.

We immediately obtain a corresponding bound on the angle-averaged extinction cross section per unit volume of a quasistatic particle [77],

$$\frac{\sigma_{\mathrm{ext}}}{V} = \frac{2\pi}{\lambda} \mathrm{Im}\left(\frac{\mathrm{Tr}(\boldsymbol{\alpha})}{3V}\right), \tag{85}$$

which is a measure of the efficiency at which a particle scatters and absorbs light. This bound reads as

$$\frac{\sigma_{\mathrm{ext}}}{V} \le \frac{2\pi}{\lambda} \max_{0 \le u \le 1} \left\{ \mathrm{Im}\left(\alpha^{\mathrm{BM}}(u)\right), \mathrm{Im}\left(\alpha^{\mathrm{DCS2}}(u)\right) \right\}, \tag{86}$$

and improves on the bounds by Miller *et al.* [72], which follow from the BM bounds. The (albeit typically small) improvement over these previously derived bounds is obtained if the maximum corresponds to a point on the arc $\alpha^{\mathrm{DCS2}}(u)$ with $u \in (0, 1)$. For example, this is the case for materials with a large negative real part of the susceptibility, i.e., metals, which give the largest values of the extinction cross section per unit volume. Ideally, to maximize the absorption, one chooses a metal with a small imaginary part of the susceptibility.

V. SUMMARY AND CONCLUSIONS

We study the range of effective complex permittivities of a three-dimensional isotropic composite material made from two isotropic phases. We start from the well-known Bergman-Milton bounds, which bound the effective complex permittivity by two circular arcs in the complex plane. In the first step, we show that several points on one of these arcs are attained by a specific class of hierarchical laminates. Furthermore, on the basis of numerical calculations, we show that there is a natural way of interpolating between these laminates, which results in laminates approaching the arc in the gaps between these points. We then show, using established variational methods, that the second arc can be replaced by an optimal bound that corresponds to assemblages of doubly coated spheres. Using this result, we derive corresponding bounds on the angle-averaged polarizability and the extinction cross section of small particles. While we focus on bounds using the quasistatic approximation, our results should be a useful benchmark for future bounds that might be more generally valid. For example, bounds on the absorption and scattering of radiation by particles of general shape and valid at any frequency have been derived in Ref. [73]. While these bounds are quite tight, they are not as tight as our bounds in the quasistatic limit. This shows that there is room for improvement, perhaps using some sort of hybrid bounding method.

ACKNOWLEDGMENTS

C.K. and G.W.M. are grateful to the National Science Foundation for support through the Research Grant No. DMS-1814854. O.D.M. was supported by the Air Force Office of Scientific Research under Award No. FA9550-17-1-0093. O.D.M. and G.W.M. thank the Korean Advanced Institute of Science and Technology (KAIST) mathematical research station (KMRS), where this work was initiated, for support through a chair professorship to G.W.M. We also thank Aaron Welters (Florida Institute of Technology) for providing some additional early references to the BM bounds in the wider context of Stieltjes functions.

[1] G. W. Milton, *The Theory of Composites*, Cambridge Monographs on Applied and Computational Mathematics Vol. 6, edited by P. G. Ciarlet, A. Iserles, Robert V. Kohn, and M. H. Wright (Cambridge University Press, Cambridge, 2002).

[2] S. A. Tretyakov, A personal view on the origins and developments of the metamaterial concept, J. Opt. **19**, 013002 (2016).

[3] M. Kadic, G. W. Milton, M. van Hecke, and M. Wegener, 3D metamaterials, Nat. Rev. Phys. **1**, 198 (2019).

[4] D. J. Bergman, Exactly Solvable Microscopic Geometries and Rigorous Bounds for the Complex Dielectric Constant of a Two-Component Composite Material, Phys. Rev. Lett. **44**, 1285 (1980).

[5] G. W. Milton, Bounds on the complex dielectric constant of a composite material, Appl. Phys. Lett. **37**, 300 (1980).

[6] G. W. Milton, Bounds on the complex permittivity of a two-component composite material, J. Appl. Phys. **52**, 5286 (1981).

[7] G. W. Milton, Bounds on the transport and optical properties of a two-component composite material, J. Appl. Phys. **52**, 5294 (1981).

[8] D. J. Bergman, Rigorous bounds for the complex dielectric constant of a two-component composite, Ann. Phys. (N.Y.) **138**, 78 (1982).

[9] A. V. Cherkaev and L. V. Gibiansky, Variational principles for complex conductivity, viscoelasticity, and similar problems in media with complex moduli, J. Math. Phys. **35**, 127 (1994).

[10] L. Tartar, in *Computing Methods in Applied Sciences and Engineering: Third International Symposium, Versailles, France, December 5–9, 1977*, Lecture Notes in Mathematics Vol. 704, edited by R. Glowinski and J.-L. Lions (Springer-Verlag, Berlin, 1979), p. 364. English translation in *Topics in the Mathematical Modelling of Composite Materials*, edited by A. Cherkaev and R. Kohn, p. 9.

[11] K. A. Lurie and A. V. Cherkaev, Accurate estimates of the conductivity of mixtures formed of two materials in a given proportion (two-dimensional problem), Doklady Akademii Nauk SSSR, **264**, 1128 (1982), English translation in Soviet Phys. Dokl. **27**, 461–462 (1982).

[12] K. A. Lurie and A. V. Cherkaev, Exact estimates of conductivity of composites formed by two isotropically conducting media taken in prescribed proportion, Proc. R. Soc. Edinburgh Sect. A **99**, 71 (1984).

[13] F. Murat and L. Tartar, in *Les méthodes de l'homogénéisation: Théorie et Applications en Physique*, Collection de la Direction des études et recherches d'Électricité de France Vol. 57 (Eyrolles, Paris, 1985), p. 319. English translation in *Topics in the Mathematical Modelling of Composite Materials*, edited by A. Cherkaev and R. Kohn, p. 139.

[14] L. Tartar, in *Ennio de Giorgi Colloquium: Papers Presented at a Colloquium Held at the H. Poincaré Institute in November 1983*, Pitman Research Notes in Mathematics Vol. 125, edited by P. Krée (Pitman Publishing Ltd., London, 1985), p. 168.

[15] L. V. Gibiansky and G. W. Milton, On the effective viscoelastic moduli of two-phase media. I. Rigorous bounds on the complex bulk modulus, Proc. R. Soc. A **440**, 163 (1993).

[16] D. J. Bergman, The dielectric constant of a composite material—A problem in classical physics, Phys. Rep. **43**, 377 (1978).
[17] A. M. Dykhne, Conductivity of a two-dimensional two-phase system, Zhurnal Eksperimental'noi i Teoreticheskoi Fiziki, **59**, 110 (1970), English translation in Sov. Phys. JETP **32**, 63–65 (1971).
[18] G. W. Milton, *Theoretical studies of the transport properties of inhomogeneous media*, Unpublished report TP/79/1 (University of Sydney, Sydney, 1979).
[19] K. M. Golden and G. C. Papanicolaou, Bounds for effective parameters of heterogeneous media by analytic continuation, Commun. Math. Phys. **90**, 473 (1983).
[20] R. C. McPhedran and G. W. Milton, Inverse transport problems for composite media, Mater. Res. Soc. Symp. Proc. **195**, 257 (1990).
[21] E. Cherkaeva and K. M. Golden, Inverse bounds for microstructural parameters of composite media derived from complex permittivity measurements, Waves Random Media **8**, 437 (1998).
[22] O. Mattei and G. W. Milton, Bounds for the response of viscoelastic composites under antiplane loadings in the time domain, in Ref. [23], pp. 149–178, see also arXiv:1602.03383 [math-ph].
[23] G. W. Milton, (editor), *Extending the Theory of Composites to Other Areas of Science* (Milton-Patton, Salt Lake City, 2016).
[24] L. D. Landau and E. M. Lifshitz, *Electrodynamics of Continuous Media*, Landau and Lifshitz Course of Theoretical Physics Vol. 8 (Pergamon, New York, 1984), Chap. 82, p. 279.
[25] J. D. Jackson, *Classical Electrodynamics* (Wiley, New York, 1999), 3rd ed.
[26] G. A. Baker, Jr., and P. R. Graves-Morris, *Padé Approximants: Basic Theory. Part I. Extensions and Applications. Part II, Encyclopedia of Mathematics and its Applications* (Addison-Wesley, Reading, 1981), Vol. 13 & 14.
[27] N. I. Akhiezer and I. M. Glazman, *Theory of Linear Operators in Hilbert Space* (Dover, New York, 1993).
[28] A. Bernland, A. Luger, and M. Gustafsson, Sum rules and constraints on passive systems, J. Phys. A **44**, 145205 (2011).
[29] M. Cassier and G. W. Milton, Bounds on Herglotz functions and fundamental limits of broadband passive quasi-static cloaking, J. Math. Phys. **58**, 071504 (2017).
[30] M. Gustafsson and D. Sjöberg, Sum rules and physical bounds on passive metamaterials, New J. Phys. **12**, 043046 (2010).
[31] D. J. Bergman, Hierarchies of Stieltjes functions and their application to the calculation of bounds for the dielectric constant of a two-component composite medium, SIAM J. Appl. Math. **53**, 915 (1993).
[32] M. G. Krein and P. Rekhtman, Concerning the Nevanlinna-Pick problem, Trans. Odessa Gas. University **2**, 63 (1938).
[33] P. Henrici and P. Pflüger, Truncation error estimates for Stieltjes functions, Numer. Math. **9**, 120 (1966).
[34] W. B. Gragg, Truncation error bounds for *g*-fractions, Numer. Math. **11**, 370 (1968).
[35] M. G. Krein and A. A. Nudel'man, *The Markov Moment Problem and Extremal Problems*, Translations of Mathematical Monographs Vol. 50 (American Mathematical Society, Providence, 1974), p. 182.
[36] Z. Hashin and S. Shtrikman, A variational approach to the theory of the effective magnetic permeability of multiphase materials, J. Appl. Phys. **33**, 3125 (1962).
[37] S. M. Stigler, Stigler's law of eponymy, Trans. New York Acad. Sci. **39**, 147 (1980).
[38] K. Schulgasser, Bounds on the conductivity of statistically isotropic polycrystals, J. Phys. C **10**, 407 (1977).
[39] M. J. Beran, Use of the variational approach to determine bounds for the effective permittivity in random media, Il Nuovo Cimento (1955–1965) **38**, 771 (1965).
[40] G. W. Milton, Bounds on the Electromagnetic, Elastic, and Other Properties of Two-Component Composites, Phys. Rev. Lett. **46**, 542 (1981).
[41] S. Torquato, Ph.D. thesis, State University of New York, Stony Brook, NY, 1980.
[42] S. Torquato and G. Stell, Bounds on the effective thermal conductivity of a dispersion of fully penetrable spheres, Int. J. Eng. Sci. **23**, 375 (1985).
[43] M. Avellaneda, A. V. Cherkaev, K. A. Lurie, and G. W. Milton, On the effective conductivity of polycrystals and a three-dimensional phase-interchange inequality, J. Appl. Phys. **63**, 4989 (1988).
[44] L. V. Gibiansky and S. Torquato, Connection between the conductivity and bulk modulus of isotropic composite materials, Proc. R. Soc. A **452**, 253 (1996).
[45] K. Schulgasser, On a phase interchange relationship for composite materials, J. Math. Phys. **17**, 378 (1976).
[46] V. Nesi, Multiphase interchange inequalities, J. Math. Phys. **32**, 2263 (1991).
[47] V. V. Zhikov, Estimates for the homogenized matrix and the homogenized tensor, Uspekhi Matematicheskikh Nauk **46(3)**, 49 (1991), English translation in Russ. Math. Surv. **46(3)**, 65 (1991)
[48] J. B. Keller, A theorem on the conductivity of a composite medium, J. Math. Phys. **5**, 548 (1964).
[49] G. W. Milton, On characterizing the set of possible effective tensors of composites: The variational method and the translation method, Commun. Pure Appl. Math. **43**, 63 (1990).
[50] G. W. Milton, P. Seppecher, and G. Bouchitté, Minimization variational principles for acoustics, elastodynamics and electromagnetism in lossy inhomogeneous bodies at fixed frequency, Proc. R. Soc. A **465**, 367 (2009).
[51] G. W. Milton and J. R. Willis, Minimum variational principles for time-harmonic waves in a dissipative medium and associated variational principles of Hashin-Shtrikman type, Proc. R. Soc. A **466**, 3013 (2010).
[52] G. W. Milton, Bounds on complex polarizabilities and a new perspective on scattering by a lossy inclusion, Phys. Rev. B **96**, 104206 (2017).
[53] S. Torquato, *Random Heterogeneous Materials: Microstructure and Macroscopic Properties*, Interdisciplinary Applied Mathematics Vol. 16 (Springer-Verlag, Berlin, 2002).
[54] A. V. Cherkaev, *Variational Methods for Structural Optimization*, Applied Mathematical Sciences Vol. 140 (Springer-Verlag, Berlin, 2000).

[55] L. Tartar, *The General Theory of Homogenization: A Personalized Introduction*, Lecture Notes of the Unione Matematica Italiana Vol. 7 (Springer-Verlag, Berlin, 2009).

[56] K. M. Golden and G. C. Papanicolaou, Bounds for effective parameters of multicomponent media by analytic continuation, J. Stat. Phys. **40**, 655 (1985).

[57] K. M. Golden, Bounds on the complex permittivity of a multicomponent material, J. Mech. Phys. Solids **34**, 333 (1986).

[58] D. J. Bergman, in *Homogenization and Effective Moduli of Materials and Media*, The IMA Volumes in Mathematics and its Applications Vol. 1, edited by J. L. Ericksen, D. Kinderlehrer, R. V. Kohn, and J.-L. Lions (Springer-Verlag, Berlin, 1986), p. 27.

[59] G. W. Milton, Multicomponent composites, electrical networks and new types of continued fraction. I, Commun. Math. Phys. **111**, 281 (1987).

[60] G. W. Milton, Multicomponent composites, electrical networks and new types of continued fraction. II, Commun. Math. Phys. **111**, 329 (1987).

[61] G. W. Milton and K. M. Golden, Representations for the conductivity functions of multicomponent composites, Commun. Pure Appl. Math. **43**, 647 (1990).

[62] A. Gully, J. Lin, E. Cherkaev, and K. M. Golden, Bounds on the complex permittivity of polycrystalline materials by analytic continuation, Proc. R. Soc. A **471**, 20140702 (2015).

[63] G. W. Milton and J. G. Berryman, On the effective viscoelastic moduli of two-phase media. II. Rigorous bounds on the complex shear modulus in three dimensions, Proc. R. Soc. A **453**, 1849 (1997).

[64] L. V. Gibiansky, G. W. Milton, and J. G. Berryman, On the effective viscoelastic moduli of two-phase media. III. Rigorous bounds on the complex shear modulus in two dimensions, Proc. R. Soc. A **455**, 2117 (1999).

[65] L. V. Gibiansky and R. S. Lakes, Bounds on the complex bulk modulus of a two-phase viscoelastic composite with arbitrary volume fractions of the components, Mech. Mater. **16**, 317 (1993).

[66] S. Glubokovskikh and B. Gurevich, Optimal bounds for attenuation of elastic waves in porous fluid-saturated media, J. Acoust. Soc. Am. **142**, 3321 (2017).

[67] J. C. Maxwell, *A Treatise on Electricity and Magnetism* (Clarendon, Oxford, 1873), p. 371, article 322.

[68] G. W. Milton, in *Continuum Models and Discrete Systems*, Interaction of Mechanics and Mathematics Series, Longman, Essex Vol. 1 edited by G. A. Maugin (Longman Scientific and Technical, Harlow, 1990), p. 60.

[69] L. V. Gibiansky, in *Homogenization*, Series on Advances in Mathematics for Applied Sciences Vol. 50, edited by V. Berdichevsky, V. V. Zhikov, and G. C. Papanicolaou (World Scientific, Singapore, 1999), p. 214.

[70] L. Tartar, in *Nonlinear Analysis and Mechanics, Heriot–Watt Symposium, Volume IV*, Research Notes in Mathematics Vol. 39, edited by R. J. Knops (Pitman, London, 1979), p. 136.

[71] G. W. Milton, R. C. McPhedran, and D. R. McKenzie, Transport properties of arrays of intersecting cylinders, Appl. Phys. **25**, 23 (1981).

[72] O. D. Miller, C. W. Hsu, M. T. H. Reid, W. Qiu, B. G. DeLacy, J. D. Joannopoulos, M. Soljačić, and S. G. Johnson, Fundamental Limits to Extinction by Metallic Nanoparticles, Phys. Rev. Lett. **112**, 123903 (2014).

[73] O. D. Miller, A. G. Polimeridis, M. T. H. Reid, C. W. Hsu, B. G. DeLacy, J. D. Joannopoulos, M. Soljačić, and S. G. Johnson, Fundamental limits to optical response in absorptive systems, Opt. Express **24**, 3329 (2016).

[74] M. Gustafsson, K. Schab, L. Jelinek, and M. Capek, Upper bounds on absorption and scattering, New J. Phys. **22**, 073013 (2020).

[75] Z. Kuang, L. Zhang, and O. D. Miller, Maximal single-frequency electromagnetic response, arXiv:2002.00521 [physics.optics] (2020).

[76] S. Molesky, P. Chao, W. Jin, and A. W. Rodriguez, Global $\mathbb{T}$ operator bounds on electromagnetic scattering: Upper bounds on far-field cross sections, Phys. Rev. Res. **2**, 033172 (2020).

[77] C. F. Bohren and D. R. Huffman, *Absorption and Scattering of Light by Small Particles* (Wiley, New York, 1988).